GENERALIZED INTEGRATION TECHNIQUES FOR HIGH-SENSITIVITY GNSS RECEIVERS AFFECTED BY OSCILLATOR PHASE NOISE

David Gómez-Casco *José A. López-Salcedo* *Gonzalo Seco-Granados*

Dpt. Telecommunications and Systems Engineering
Universitat Autònoma de Barcelona (UAB), Spain

ABSTRACT

This paper addresses the use of generalized correlations in the context of High-Sensitivity Global Navigation Satellite System (HS-GNSS) receivers. Generalized correlations are also referred to as post-detection integration (PDI) techniques or simply as non-coherent integration methods. The contributions of this work are twofold. On the one hand, a novel PDI method is presented, which improves the performance of methods found in the literature for small errors of the frequency offset. On the other hand, an exhaustive comparative performance analysis is provided between the proposed technique and the existing ones in the presence of phase noise coming from the local oscillator. To this end, results have been obtained for two different clocks, namely a temperature compensated crystal oscillator (TCXO) and an oven-controlled crystal oscillator (OCXO). In both cases, the proposed technique outperforms the existing ones.

Index Terms— High-sensitivity GNSS, non-coherent integration, phase noise, TCXO, OCXO.

1. INTRODUCTION

Severe attenuation limits the applicability of GNSS receivers in many scenarios where positioning information would be highly desirable [1]. In those scenarios, the integration time in the receiver must be dramatically increased to accumulate enough energy to be able to detect the signal. The total integration time is determined by a coherent integration period that is repeated several times. This repetition and the subsequent combination (in a way to be determined) of the results of the coherent integrations are usually referred to as post-detection integration (PDI) or non-coherent accumulation. The increase of the coherent integration time is in theory the most effective way to enhance sensitivity, but in practice this cannot be done without limit since the residual frequency offsets and the phase noise restrict the gains of coherent integration. Then, one has to resort to PDI techniques to further increase the total integration time and to obtain additional improvements in sensitivity. Although the non-coherent accumulation is less effective than the coherent integration in ideal conditions (*i.e.* when additive thermal noise is the only disturbance), they have the advantage of being potentially robust against residual frequency errors and phase noise [2, 3].

Different techniques or strategies have been proposed in order to improve the sensitivity of non-coherent integration (see a review in [1, 3, 4]). However, the question about which is the best method to perform the non-coherent integration under practical conditions remains open. One of the most relevant practical conditions, often overlooked in theoretical studies, is that the GNSS receiver clock introduces an error in the signal, which is usually time-varying. This error is known as phase noise and it results in small random fluctuations or uncertainties in the phase of a GNSS signal. The main problem of this noise is that it limits the duration of the coherent integration time.

In this paper, a new PDI technique is proposed and extensively analyzed under realistic settings (with phase noise coming from two different clocks) together with other PDI techniques found in the literature. Furthermore, the maximum values of the coherent integration time for different clock types are determined.

2. SIGNAL MODEL

The signal received by a GNSS receiver can be expressed in baseband as

$$r(n) = \sum_{p=1}^{P} A_p b_p(n-\tau_p) s_p(n-\tau_p) e^{j(2\pi f_{d,p} n + \theta_p)} + \omega(n), \quad (1)$$

where P is the number of GNSS satellites, $s_p(n)$ is the pseudo-random code sequence of the pth satellite , A_p is the received amplitude, $b_p(n)$ is the unknown data information, τ_p is the code delay from satellite to receiver, $f_{d,p}$ is the Doppler frequency owing to movement of the satellite and the receiver clock, θ_p is the phase of the received signal, and $\omega(n)$ is the complex additive white Gaussian noise (AWGN). In order to acquire the different satellites currently in view, the received signal is correlated for each pseudo-random sequence of the P satellites. If a satellite is in view, the result of the correlation between the received signal and the pseudo-random sequence of this satellite is a high peak. However, many times it is not possible to see this peak due to the severe attenuation of the received signal. As a result, the level of the noise is higher than the value of the peak. In order to reduce the effect of noise the coherent integration is performed. The coherent integration consists in the sum of different correlations of length L computed from different time instants of the received signal. The output of the coherent integration process can be expressed as

$$R_k(\Delta\tau, \Delta f) = \sum_{m=0}^{N_{coh}-1} \sum_{n=1}^{L} r(n+mL+kLN_{coh}) x^*(n), \quad (2)$$

with

$$x(n) = s_l(n-\tau) e^{j2\pi f_d n}, \quad (3)$$

where $x(n)$ is the pseudo-random sequence of the lth satellite with τ and f_d trial values of the code delay and the Doppler frequency of the lth satellite, respectively; N_{coh} is the number of code periods of length L inside a coherent integration time, $\Delta f = f_d - f_{d,p}$ is the residual frequency offset, $\Delta\tau = \tau - \tau_p$ is the residual delay offset,

978-1-4673-7802-4/16/$31.00 ©2016 IEEE

$k = 1, ..., N_{nc}$ and N_{nc} is the number of non-coherent integrations. After that, the metric Z_X is generated by applying a PDI technique, which is obtained by using a non-linear function to the output of the coherent integration, to further reduce the effect of noise.

The metric Z_X is evaluated for different values of $\Delta\tau$ and Δf, but we omit the explicit dependence for convenience. In a real receiver this process is done for all the P satellites. However, in this work, we perform this process only for the lth satellite because it is enough to analyze the performance of the PDI techniques. In this sense, the problem of acquiring the satellite can be modelled by two hypotheses: under H_0 the signal is absent (*i.e.* $A_l = 0$) and under H_1 the signal is present (*i.e.* $A_l > 0$) for a certain value of τ and f_d. The distinction between the two hypotheses can be performed comparing the maximum value of Z_X with a given threshold [1]. Thereby, if the maximum value of Z_X exceeds this threshold, the signal is declared present and a coarse estimation of the delay and the Doppler frequency of the received signal is obtained.

3. PDI TECHNIQUES

In GNSS receivers, the most commonly used technique for non-coherent integration is the so-called non-coherent PDI (NPDI) [5] and it can be defined by

$$Z_{\text{NPDI}} = \sum_{k=1}^{N_{nc}} |R_k(\Delta\tau, \Delta f)|^2. \tag{4}$$

Using the absolute value of the outputs of the coherent integration the effect of the changing signal phase, due to the frequency offset, is eliminated, and thus the outputs of several coherent integration intervals can be combined. Alternatively, Differential PDI (DPDI) [6] can be used and it can be expressed as

$$Z_{\text{DPDI}} = \left| \sum_{k=2}^{N_{nc}} R_k(\Delta\tau, \Delta f) R^*_{k-1}(\Delta\tau, \Delta f) \right|. \tag{5}$$

The basis of DPDI is that the noise components of two coherent correlations are uncorrelated one with each other, while the signal components are strongly correlated. Another alternative is the Generalized PDI Truncated (GPDIT) [7, 8]. The fundamental aspect of this technique is that it combines the term corresponding to NPDI with the one corresponding to DPDI, which may lead to a better detection probability than NPDI and DPDI. The GPDIT is expressed as

$$\begin{aligned} Z_{\text{GPDIT}} &= \sum_{k=1}^{N_{nc}} |R_k(\Delta\tau, \Delta f)|^2 \\ &\quad + 2 \left| \sum_{k=2}^{N_{nc}} R_k(\Delta\tau, \Delta f) R^*_{k-1}(\Delta\tau, \Delta f) \right|. \end{aligned} \tag{6}$$

An additional method has been proposed in [9, 10]. The main idea behind this method is to combine the term corresponding to the NPDI with a new term. This new term is referred to as squaring detector (SD), and it is the sum the squared values of the outputs of the coherent integrator, as it is shown in the following equation.

$$Z_{\text{NPDISD}} = \sum_{k=1}^{N_{nc}} |R_k(\Delta\tau, \Delta f)|^2 + \left| \sum_{k=1}^{N_{nc}} R_k(\Delta\tau, \Delta f)^2 \right|. \tag{7}$$

The last method, which is the one that we propose and referred herein as GPDITSD, is the result of taking into account the terms of both the GPDIT and the SD. The rationale for this will be explained later on, when its performance is analysed.

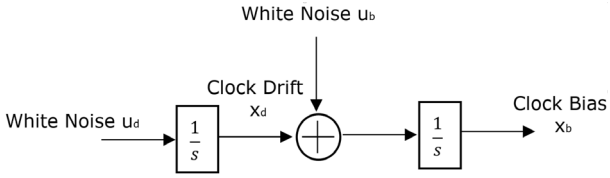

Fig. 1. Clock error modeling.

$$\begin{aligned} Z_{\text{GPDITSD}} &= \sum_{k=1}^{N_{nc}} |R_k(\Delta\tau, \Delta f)|^2 \\ &\quad + 2 \left| \sum_{k=2}^{N_{nc}} R_k(\Delta\tau, \Delta f) R^*_{k-1}(\Delta\tau, \Delta f) \right| \\ &\quad + \left| \sum_{k=1}^{N_{nc}} R_k(\Delta\tau, \Delta f)^2 \right|. \end{aligned} \tag{8}$$

4. PHASE NOISE

One of the main limitations of HS-GNSS receivers is caused by clock instabilities, which translate into random deviations of the instantaneous phase, often referred to as *phase noise* [11]. As a result, the coherent integration time cannot be increased without bound because there is a risk of signal cancellation.

The clock error can be modelled and generated using a 2-state system. This clock model was developed in [12] and later also applied in [13]. It is depicted in Fig. 1, where u_b and u_d are two independent noise components, x_d is the clock drift, and x_b is the clock bias. Thus, x_b represents the random fluctuations that exhibits the GNSS received signal at the front-end output. The noises u_b and u_d are Gaussian noise with mean zero and variance $\frac{S_f}{\Delta T}$ and $\frac{S_g}{\Delta T}$, respectively. The parameter ΔT is the sampling time. A representation of the clock characteristics is given by the spectral parameters: S_f and S_g, which are related to other coefficients h_0 and h_{-2} as follows:

$$S_f \approx \frac{h_0}{2} \tag{9}$$

$$S_g \approx 2\pi^2 h_{-2}. \tag{10}$$

Coefficients h_0 and h_{-2} correspond the white frequency noise and the random walk frequency noise terms, respectively, and they are used to characterize different types and qualities of clocks. In our simulations, we have used two clocks, namely, a TCXO and a OCXO. The power of phase noise introduced by a TCXO clock is larger than the power of phase noise introduced by a OCXO clock. More precisely, the parameters used for TCXO clock and OCXO are given by [14] and they are shown in the Table 1.

5. PERFORMANCE ANALYSIS

The probability distributions of the metrics defined in (5), (6) and (8) are not known in a closed-form and many approximations are needed if one wants to attempt a theoretical performance analysis. A big handicap is that the covariance between the individual terms in

	h_0 [seconds]	h_{-2} [seconds]
TCXO	9.43e-20	3.8e-21
OCXO	3.4e-22	1.3-24

Table 1. Clock parameters.

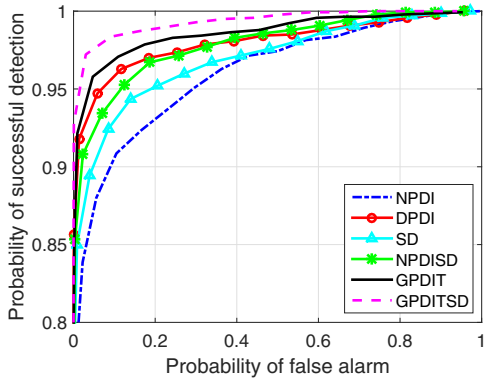

Fig. 2. ROC curves for C/N0=20 dBHz, coherent integration time=100 ms, N_{nc}=7 and Δf=0 Hz.

(6) and (8) are also not known. Moreover, the addition of the phase noise in a theoretical analysis is not feasible. Since we are interested in assessing the performance of the different methods in the most accurate possible way, we have resorted to extensive numerical simulations.

The first subsection deals only with the presence of AWGN, but not phase noise, while the second subsection considers both AWGN and phase noise. The Receiver Operating Characteristics (ROC) curve is used to analyze the performance of the detection methods. Simulations have been performed using the Galileo E1 signal [15] for different values of carrier-to-noise ratio (C/N0). In addition, HS-GNSS receivers are able to detect weak signals by extending a large coherent integration time and using a small number of N_{nc} [16]. For this reason, we apply the same approach in our simulations using a long coherent time and applying a small number of N_{nc}.

5.1. Simulation without phase noise

Fig. 2 shows that the proposed GPDITSD offers a significant gain in terms of probability of detection vs. probability of false alarm when the frequency offset is zero. The key aspect of this method is that it combines the terms corresponding to NPDI with both DPDI and SD.

Comparing the performance of the individual terms that form the GPDITSD, the following conclusions can be drawn:

- SD outperforms NPDI.
- DPDI outperforms NPDI and SD.
- NPDISD outperforms NPDI and SD.
- GPDIT outperforms NPDISD.

In the first simulation, the frequency offset of the incoming signal was set to 0 Hz. The following simulation considers the frequency offset to be a uniform random variable in the range [-50Hz, 50Hz]. It can be seen in Fig. 3 that the SD method suffers significant degradation in presence of frequency offset. Due to this degradation, GPDIT turns out to be the best performing technique, unlike the

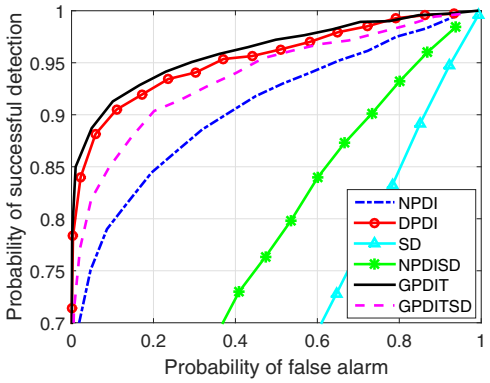

Fig. 3. ROC curves for C/N0=20 dBHz, coherent integration time=100 ms, N_{nc}=7 and Δf=+/- 50 Hz.

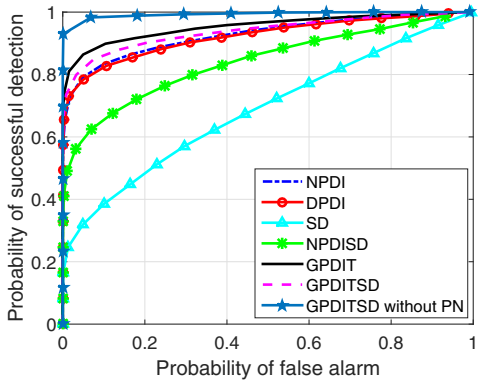

Fig. 4. ROC curves for C/N0=20 dBHz, coherent integration time=100 ms, N_{nc}=7, Δf=0 Hz and using a TCXO ("without PN" means "without phase noise").

case with no frequency offset, where GPDITSD outperformed the rest of detectors. The comparison between GPDITSD and GPDIT reveals that there is a certain value of frequency offset below which GPDITSD is advantageous; and above this value, GPDIT is preferable. This is an important result because different applications, depending on the dynamics of the receiver, have different Doppler uncertainty, and hence one technique may be more appropriate than the other. Extensive simulations have shown that this thresholding frequency offset value is 1Hz for a coherent integration time equal to 100 ms.

5.2. Simulation with phase noise

The phase noise caused by TXCO clock is introduced in the simulation, as shown in Fig. 4. The ROC of the methods is obviously degraded with respect to the case without phase noise. Nevertheless, it is still possible to use a relatively long integration time (*i.e.* 100 ms) with this TCXO.

We recall that, when the frequency offset is null, the method that has the best performance is the GPDITSD in absence of phase noise. However, when phase noise is added to a large extent (as it is the case with a TCXO), the GPDIT turns out to be the best method even when the frequency offset is zero. This occurs because the

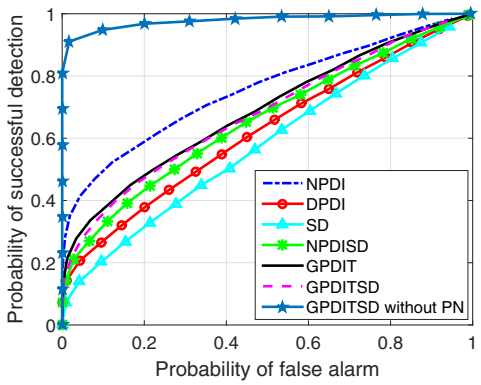

Fig. 5. ROC curves for C/N0=15 dBHz, coherent integration time=500 ms, N_{nc}=4, Δf=0 Hz and using a TCXO.

SD term suffers a severe degradation, which was a shortcoming not identified in the existing papers [9, 10]. Moreover, the DPDI method also experiences a breakdown due to the phase noise because, unlike the case without phase noise (Fig. 2), it has a very similar ROC to the standard NPDI. As a consequence, given the marginal advantage of GPDIT with respect to NPDI, but its higher complexity, we can conclude that NPDI is the most robust method in case of large phase noise. Furthermore, the results in Fig. 5 confirm that a coherent time of 500 ms is not feasible with a TCXO; and in any case, the NPDI would be the method providing the least degraded ROC.

An OCXO is used for the results in Fig. 6. In this case, the coherent integration is increased to 1 second. The results show that coherent integrations of 1 second are perfectly feasible with this type of clock. As the phase noise is small, the GPDITSD offers the best performance, and very similar to the case without phase noise. Actually, the SD term is almost not degraded using this clock unlike the case with TCXO, which is the reason why the GPDITSD maintains its advantage.

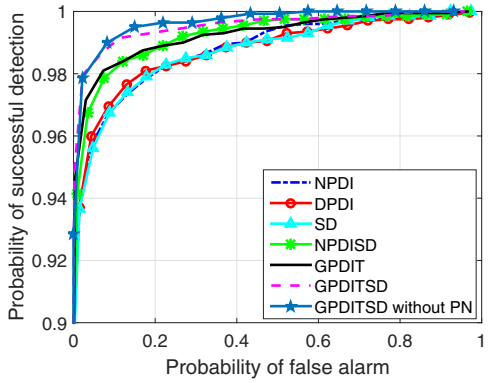

Fig. 6. ROC curves for C/N0=12 dBHz, coherent integration time=1000 ms, N_{nc}=4, Δf=0 Hz and using a OCXO.

6. CONCLUSIONS

We have proposed a novel generalized integration method, named GPDITSD, to enhance the sensitivity of GNSS receivers. It is the combination of different variants of non-coherent and differential detectors. We have analyzed the performance of several detectors under several conditions of frequency offset error and assuming receivers with a standard (TCXO) or with a average-to-good (OCXO) quality clocks. The simulation results have delimitated the conditions under which one technique outperforms the others. In general, the TCXO limits the coherent correlation interval to about 100 ms, and the large phase noise wipes outs the advantage of all differential and squaring detectors, leaving the standard non-coherent detector as the best option. On the other hand, the OCXO permits the use of coherent integration times as long as 1 second, and the advanced detectors behave much better than the NPDI. In particular, our proposed technique outperforms all the others when the frequency uncertainty is below a given threshold that has also been quantified.

7. REFERENCES

[1] G. Seco-Granados, J.A. Lopez-Salcedo, D. Jimenez-Banos, and G. Lopez-Risueno, "Challenges in indoor global navigation satellite systems: Unveiling its core features in signal processing," *IEEE Signal Processing Magazine*, vol. 29, no. 2, pp. 108–131, March 2012.

[2] C. Yang, M. Miller, E. Blasch, and T. Nguyen, "Comparative study of coherent, non-coherent, and semi-coherent integration schemes for GNSS receivers," in *ION Annual meeting*, April 2007, pp. 572–588.

[3] F. Dovis and Tung Hai Ta, "High sensitivity techniques for GNSS signal acquisition," in *Global Navigation Satellite Systems: Signal, Theory and Applications*, Shuanggen Jin, Ed. In-Tech, 2012.

[4] E.S. Lohan, J.A. Lopez-Salcedo, and G. Seco-Granados, "Analysis of generalized post-detection integration techniques for the acquisition with pilot signals in High Sensitivity-Galileo receivers," in *ESA Colloquium on scientific and fundamental aspects of Galileo*, 2013.

[5] A. Schmid and A. Neubauer, "Differential correlation for Galileo/GPS receivers," in *IEEE International Conference on Acoustics, Speech, and Signal Processing (ICASSP)*, March 2005, vol. 3, pp. iii/953–iii/956.

[6] H. Elders-Boll and U. Dettmar, "Efficient differentially coherent code/Doppler acquisition of weak GPS signals," in *IEEE Eighth International Symposium on Spread Spectrum Techniques and Applications*, Aug 2004, pp. 731–735.

[7] G.E. Corazza and R. Pedone, "Generalized and average likelihood ratio testing for post detection integration," *IEEE Transactions on Communications*, vol. 55, no. 11, pp. 2159–2171, Nov 2007.

[8] G.E. Corazza and R. Pedone, "Maximum likelihood post detection integration methods for spread spectrum systems," in *Wireless Communications and Networking (WCNC)*, March 2003, vol. 1, pp. 227–232.

[9] S. Satyanarayana, D. Borio, and G. Lachapelle, "A non-coherent block processing architecture for standalone GNSS weak signal tracking," in *ION GNSS*, September 2011, pp. 1777–1785.

[10] D. Borio, "Non-coherent squaring detector and its application to bi-phased signals," *IET Radar, Sonar Navigation*, vol. 8, no. 4, pp. 327–335, April 2014.

[11] E. Perez Serna, S. Thombre, M. Valkama, S. Lohan, V. Syrjälä, M. Detratti, H. Hurskainen, and J. Nurmi, "Local oscillator phase noise effects on GNSS code tracking," *Inside GNSS*, 2010.

[12] P. Y. C. Hwang and R. G. Brown, *Introduction to Random Signals and Applied Kalman Filtering*, Wiley, 1992.

[13] T.S. Bruggemann, D.G. Greer, and R.A Walker, "Chip Scale Atomic Clocks: Benefits to Airborne GNSS Navigation Performance," in *International Global Navigation Satellite Systems Society Symposium*, 2006.

[14] J.T. Curran, G. Lachapelle, and C.C. Murphy, "Digital GNSS PLL Design Conditioned on Thermal and Oscillator Phase Noise," *IEEE Transactions on Aerospace and Electronic Systems*, vol. 48, no. 1, pp. 180–196, Jan 2012.

[15] European Commission, "European GNSS (Galileo) Open Service. Signal in Space Interface Control Document," 2011.

[16] L. Musumeci, F. Dovis, P. F. Silva, H. D. Lopes, and J. S. Silva, "Design of a very high sensitivity acquisition system for a space GNSS receiver," in *ION PLANS*, 2014, pp. 556–568.